

RAPID COMMUNICATION | OCTOBER 12 2011

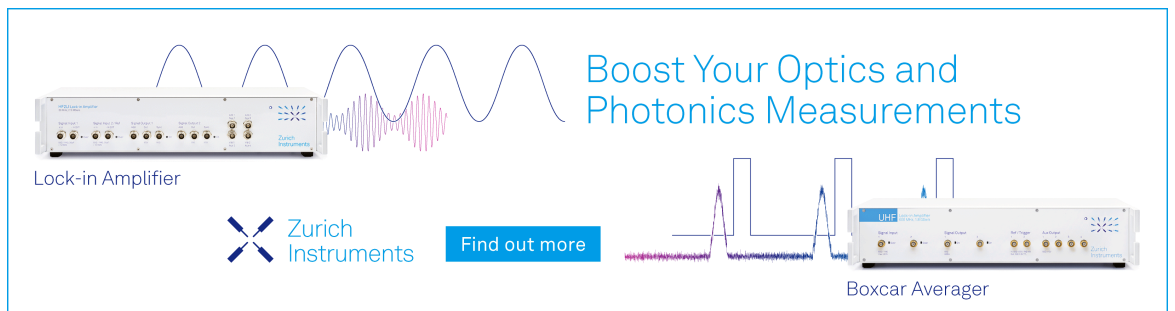
## Communication: Consistent picture of lateral subdiffusion in lipid bilayers: Molecular dynamics simulation and exact results

Gerald R. Kneller; Krzysztof Baczynski; Marta Pasenkiewicz-Gierula




*J. Chem. Phys.* 135, 141105 (2011)

<https://doi.org/10.1063/1.3651800>



Boost Your Optics and Photonics Measurements

Lock-in Amplifier

 Zurich Instruments

[Find out more](#)

Boxcar Averager

## Communication: Consistent picture of lateral subdiffusion in lipid bilayers: Molecular dynamics simulation and exact results

Gerald R. Kneller,<sup>1,2,3,a)</sup> Krzysztof Baczynski,<sup>4</sup> and Marta Pasenkiewicz-Gierula<sup>4</sup>

<sup>1</sup>Centre de Biophysique Moléculaire, CNRS, Rue Charles Sadron, 45071 Orléans, France

<sup>2</sup>Synchrotron Soleil, L'Orme de Merisiers, 91192 Gif-sur-Yvette, France

<sup>3</sup>Université d'Orléans, Chateau de la Source-Av. du Parc Floral, 45067 Orléans, France

<sup>4</sup>Faculty of Biochemistry, Biophysics and Biotechnology, Jagiellonian University, Krakow, Poland

(Received 26 July 2011; accepted 26 September 2011; published online 12 October 2011)

This communication presents a molecular dynamics simulation study of a bilayer consisting of 128 dioleoyl-sn-glycero-3-phosphocholine molecules, which focusses on the center-of-mass diffusion of the lipid molecules parallel to the membrane plane. The analysis of the simulation results is performed within the framework of the generalized Langevin equation and leads to a consistent picture of subdiffusion. The mean square displacement of the lipid molecules evolves as  $\propto t^\alpha$ , with  $\alpha$  between 0.5 and 0.6, and the fractional diffusion coefficient is close to the experimental value for a similar system obtained by fluorescence correlation spectroscopy. We show that the long-time tails of the lateral velocity autocorrelation function and the associated memory function agree well with exact results which have been recently derived by asymptotic analysis [G. Kneller, *J. Chem. Phys.* **134**, 224106 (2011)]. In this context, we define characteristic time scales for these two quantities. © 2011 American Institute of Physics. [doi:10.1063/1.3651800]

Over the last decades, a considerable amount of experimental data has been collected which gives evidence of anomalous diffusion processes in a large variety of systems. The common observation is that the mean square displacement (MSD) of a freely diffusing particle deviates from the linear form predicted by Einstein.<sup>1</sup> Defining  $W(t) \equiv \langle \{\mathbf{x}(t) - \mathbf{x}(0)\}^2 \rangle$ , where  $\mathbf{x}$  is the position of the tagged particle and  $\langle \dots \rangle$  denotes an ensemble average, one observes instead MSDs of the more general form<sup>2</sup>

$$W(t) \stackrel{t \rightarrow \infty}{\sim} 2D_\alpha t^\alpha, \quad 0 < \alpha < 2. \quad (1)$$

The regimes  $0 < \alpha < 1$  and  $1 < \alpha < 2$  are referred to as subdiffusion and superdiffusion, respectively, and the fractional diffusion constant  $D_\alpha$  has the physical dimension  $\text{length}^2/\text{time}^\alpha$ . Due to the development of fluorescence-based observation methods, such as fluorescence correlation spectroscopy (FCS) and single particle tracking (SPT) methods, anomalous diffusion processes have also been observed in biological systems, in particular, in membranes and in the cell.<sup>3-9</sup> Concerning the lateral diffusion of molecules in lipid bilayers, the observation of anomalous diffusion is, to some extent, still under debate. Computer simulations and NMR experiments on the nano- to microsecond time scale suggest that lateral subdiffusion in membranes is a transient phenomenon,<sup>10</sup> or that it does not exist at all,<sup>11</sup> although FCS experiments on the millisecond time scale clearly see this phenomenon.<sup>4</sup> The idea of this communication is to shed some light on this question by analyzing a 90 ns molecular dynamics (MD) simulation of a lipid model bilayer in the framework of the generalized Langevin equation (GLE).<sup>12</sup> For this purpose, we performed a 160 ns simulation of a

system consisting of 128 ( $8 \times 8 \times 2$ ) dioleoyl-sn-glycero-3-phosphocholine (DOPC) molecules hydrated by 3840 water molecules, using the GROMACS 3.3.1 package.<sup>13</sup> The system is shown in Fig. 1. The electrostatic interactions were evaluated using the particle-mesh Ewald summation.<sup>14</sup> For the real box, three-dimensional periodic boundary conditions with the usual minimum image convention and a cutoff of 12 Å were used. To allow for a time step of 2 fs, we applied the SHAKE algorithm<sup>15</sup> to constrain the lengths of all OH and CH bonds to their respective equilibrium values. The system was equilibrated for 70 ns and the remaining 90 ns of the MD trajectory were used for further analysis. The MD simulation was carried out at constant pressure (1 atm) and at a temperature of 310 K (37 °C), which is above the main phase transition temperature (−20 °C) for the DOPC bilayer.<sup>16</sup> Temperature and pressure of the system were controlled by the Berendsen method,<sup>17</sup> setting the corresponding relaxation times both to 0.5 ps. Here, the temperatures of the solute and the solvent were controlled independently and the applied pressure was controlled anisotropically, keeping the trace of the pressure tensor at 1 atm.

As a first analysis of the simulation, we computed the MSD for the lateral center-of-mass (CM) motion of the DOPC molecules. The MSDs of the individual molecules were estimated through the time average

$$W_j(n) \approx \frac{1}{N_t - n} \sum_{k=0}^{N_t - n - 1} (\mathbf{x}_j(k+n) - \mathbf{x}_j(k))^2, \quad (2)$$

and the results were averaged over all (physically equivalent) DOPC molecules

$$W(n) = \frac{1}{N_{\text{mol}}} \sum_{j=1}^{N_{\text{mol}}} W_j(n). \quad (3)$$

<sup>a)</sup> Author to whom correspondence should be addressed. Electronic mail: gerald.kneller@cnrs-orleans.fr.

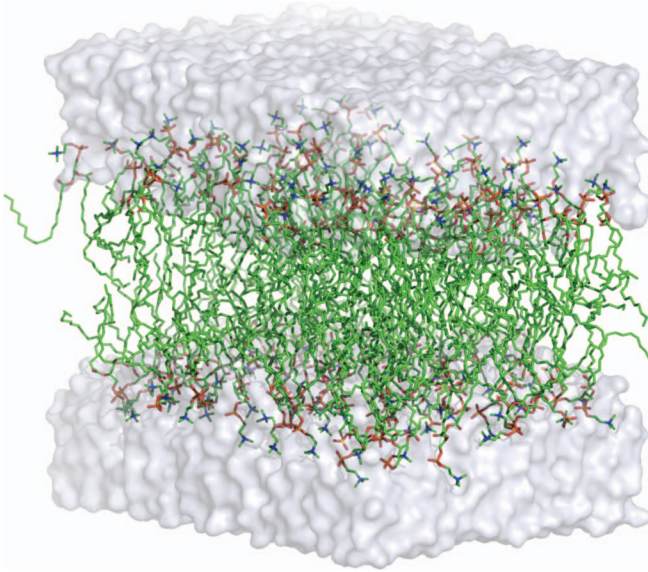


FIG. 1. Simulated system consisting of a bilayer of  $2 \times 64$  DOPC lipid molecules and 3840 water molecules (light-grey).

Here  $N_{\text{mol}}$  denotes the number of lipid molecules,  $N_t$  is the number of time steps in the MD trajectory, and  $\mathbf{x}(n) \equiv \mathbf{x}(n\Delta t)$ , with  $\Delta t$  being the sampling time step. The results for two different lag time scales (1 ns and 30 ns) are shown in Figs. 2 and 3, respectively, where dots correspond to the simulated MSDs and solid lines to the fits of expression (1). The fit parameters are  $\alpha = 0.52$ ,  $D_\alpha = 0.107 \text{ nm}^2/\text{ns}^\alpha$  for the fit in Fig. 2 and  $\alpha = 0.61$ ,  $D_\alpha = 0.101 \text{ nm}^2/\text{ns}^\alpha$  for the fit in Fig. 3. We have also performed an analysis for an intermediate lag time scale of 5 ns (not shown here), which lead to  $\alpha = 0.56$ ,  $D_\alpha = 0.110 \text{ nm}^2/\text{ns}^\alpha$ . The insets of Figs. 2 and 3 show the spread of the MSDs for the individual molecules. The rapid increase of the latter with the lag time spots the problem of statistical reliability, if the lag time becomes comparable with the length of the simulation trajectory. The form of the spread gives also a hint to appropriate stochastic models describing the observed subdiffusion, such as (ergodic) fractional Brownian motion (fBM) and the (non-ergodic) continuous time random walk.<sup>18</sup> Here, one has to make the assumption that the average over all molecules corresponds to a true ensemble average. The observed Gaussian shape of the distribution functions shown in Figs. 2 and 3 supports that the lateral subdiffusion of the DOPC molecules can be described by fBM. In recent experimental studies, both models have been used to describe experimental data for trajectories of diffusing molecules.<sup>7-9</sup> We note finally that the fractional diffusion constant found for the lateral diffusion of lipid molecules in the giant vesicles studied in Ref. 4 is  $D_\alpha = 0.088 \pm 0.007 \text{ nm}^2/\text{ns}^\alpha$  for  $\alpha = 0.74 \pm 0.08$ . Although the lipid bilayer considered in this study consisted of different lipid molecules (dilauroyl-sn-glycero-3-phosphocholine or DLPC), the measured diffusion coefficient shows that the results for  $D_\alpha$  obtained in our simulation study of DOPC are of the right order of magnitude.

In the following, we further analyze the lateral center-of-mass dynamics of the DOPC molecules in the framework of the GLE.<sup>12</sup> The velocity autocorrelation function (VACF) of a tagged molecule,  $c(t) \equiv \langle \mathbf{v}(0) \cdot \mathbf{v}(t) \rangle$ , fulfills then the integro-

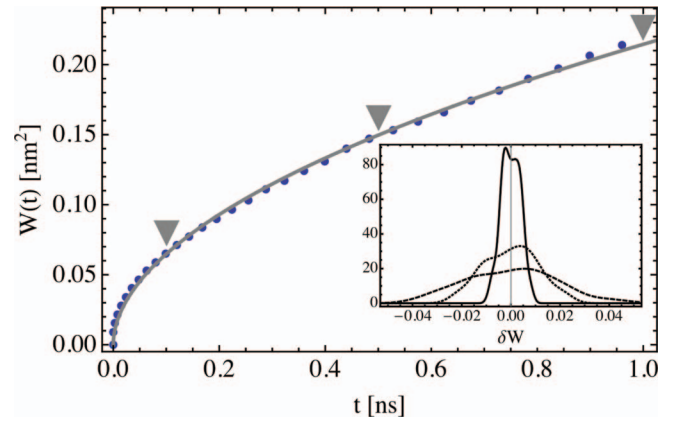


FIG. 2. Simulated molecule-averaged MSD for the lateral CM diffusion of the DOPC molecules (dots) and fit of model (1) (solid line). The fitted fractional diffusion coefficient is  $D_\alpha = 0.107 \text{ nm}^2/\text{ns}^\alpha$  for  $\alpha = 0.52$ . The inset shows the distribution of  $\delta W(t) = W_j(t) - W(t)$  for  $t = 0.1 \text{ ns}$ ,  $t = 0.5 \text{ ns}$ , and  $t = 1 \text{ ns}$  (with increasing width). In the main figure the corresponding average MSD values are indicated by triangles.

differential equation

$$\partial_t c(t) = - \int_0^t dt' \kappa(t-t')c(t'), \quad (4)$$

where  $\kappa(t)$  is the corresponding memory kernel. Formally, the latter can be derived from the microscopic Hamiltonian dynamics of the system under consideration (tagged particle plus the environment). Using that the MSD and the VACF are related through<sup>19</sup>

$$W(t) = 2 \int_0^t d\tau (t-\tau)c(\tau), \quad (5)$$

one can derive characteristic long-time tails for the VACF and its memory function,<sup>20</sup>

$$c(t) \stackrel{t \rightarrow \infty}{\sim} D_\alpha \alpha (\alpha - 1) t^{\alpha-2}, \quad (6)$$

$$\kappa(t) \stackrel{t \rightarrow \infty}{\sim} \frac{\langle \mathbf{v}^2 \rangle}{D_\alpha} \frac{\sin(\pi\alpha)}{\pi\alpha} t^{-\alpha}, \quad (7)$$

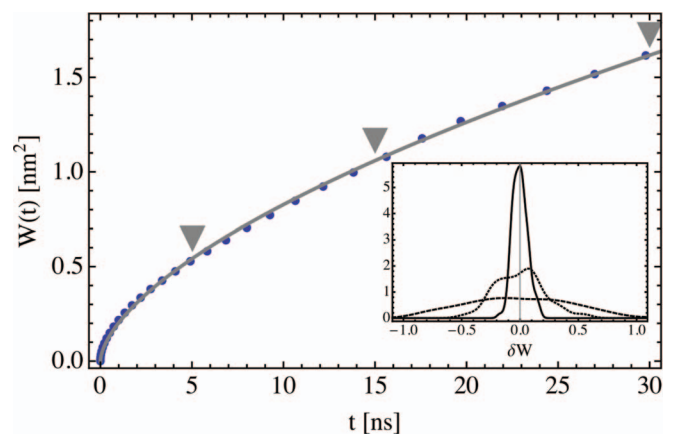


FIG. 3. As Fig. 2, but for a maximum time lag of 30 ns. Here, the fitted fractional diffusion coefficient is  $D_\alpha = 0.101 \text{ nm}^2/\text{ns}^\alpha$  for  $\alpha = 0.61$  and the inset shows the spread of the molecular MSDs at  $t = 5 \text{ ns}$ ,  $t = 15 \text{ ns}$ , and  $t = 30 \text{ ns}$ .

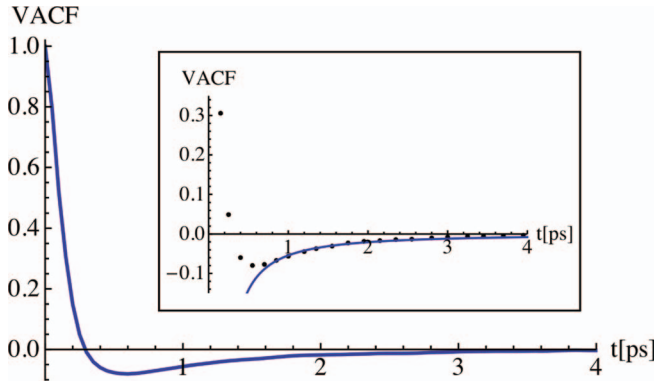


FIG. 4. Normalized simulated VACF for the lateral CM motion of the DOPC molecules. The inset shows the superposition of the simulated VACF (dots) with the long-time tail (6) (solid line). Here it is taken into account that  $c(0) = 1$ , and the characteristic time scale defined according to Eq. (11) is  $\tau_{\text{VACF}} = 0.35$  ps.

which are to be considered as necessary conditions for anomalous diffusion. Expressions (6) and (7) are also sufficient conditions in case of super- and subdiffusion, respectively. For subdiffusion, the theory predicts thus a negative long-time tail for the VACF and a positive long-time tail for the memory function. Negative values of the VACF for large time lags indicate a persistent tendency of the diffusing molecules to invert their direction of motion and thus a tendency to stay localized. In agreement with this interpretation, Eq. (4) shows that the inversion of the direction of motion is favored by positive values of the memory function. In this context, it is worthwhile noting that the VACF for fBM, which can be defined for a coarse-grained velocity, decays asymptotically also as  $t^{\alpha-2}$ , with  $c(t) < 0$ .<sup>9</sup>

To investigate the existence of a long-time tail in the VACF, we estimated the contributions of the individual molecules again through time averages

$$c_j(n) \approx \frac{1}{N_t - n} \sum_{k=0}^{N_t - n - 1} \mathbf{v}_j(k) \cdot \mathbf{v}_j(k+n) \quad (8)$$

and calculated the VACF as an average over the individual contributions,

$$c(n) = \frac{1}{N_{\text{mol}}} \sum_{j=1}^{N_{\text{mol}}} c_j(n). \quad (9)$$

The results are shown in Fig. 4, where the VACF has been normalized such that  $c(0) = 1$ . The inset shows that the computed VACF (dots) is in good agreement with the long-time tail (6) (solid line) if  $t > 1$  ps. In this comparison, the normalization of the VACF has been taken into account. The asymptotic regime of the VACF is defined with respect to a corresponding typical time scale,  $\tau_{\text{VACF}}$ . For normal diffusion, this time scale can be obtained via  $\tau_{\text{VACF}} = \int_0^\infty dt c(t)/c(0)$ . To generalize this estimation for arbitrary  $\alpha$  we use that the fractional diffusion constant can be written as<sup>20</sup>

$$D_\alpha = \frac{1}{\Gamma(1+\alpha)} \int_0^\infty dt {}_0\partial_t^{\alpha-1} c(t), \quad (10)$$

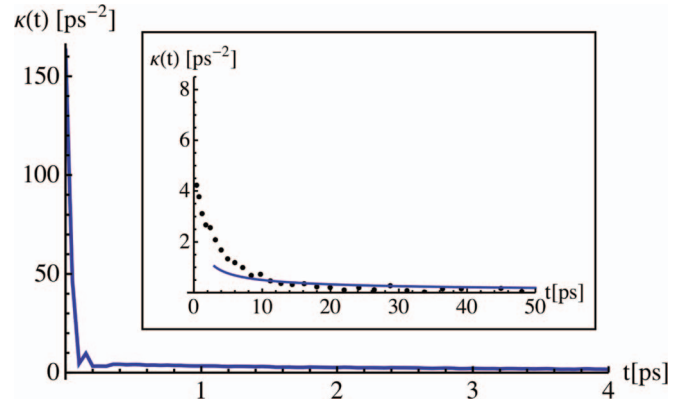


FIG. 5. Memory function associated with the VACF shown in Fig. 4. The inset shows the superposition of the calculated memory function (dots) with the corresponding long-time tail (7) (solid line). The characteristic time scale defined according to Eq. (14) is  $\tau_{\text{mem}} = 2.4$  fs.

where  $\Gamma(\cdot)$  is the Gamma function<sup>21</sup> and  ${}_0\partial_t^{\alpha-1} c(t) = d/dt \int_0^t dt' \Gamma(\alpha)^{-1} (t-t')^{\alpha-1} c(t')$  is the fractional Riemann-Liouville derivative<sup>22</sup> of order  $1 - \alpha$  of  $c(t)$ . Noting that  $c(0) = \langle \mathbf{v}^2 \rangle$ , we define

$$\tau_{\text{VACF}} = \left( \frac{D_\alpha}{\langle \mathbf{v}^2 \rangle} \right)^{1/(2-\alpha)}. \quad (11)$$

Using  $\alpha = 0.61$ ,  $D_\alpha = 0.101 \text{ nm}^2/\text{ns}^\alpha$ , and a thermal mean square velocity of  $\langle \mathbf{v}^2 \rangle = k_B T/M = 6.55 \times 10^{-3} \text{ nm}^2/\text{ps}^2$  at  $T = 310 \text{ K}$ , yields  $\tau_{\text{VACF}} = 0.35$  ps. Here  $k_B$  is the Boltzmann constant,  $T$  is the absolute temperature in Kelvin, and  $M$  is the mass of a single DOPC molecule. What exactly means  $t \gg \tau_{\text{VACF}}$  can be seen from Fig. 4, which shows that the asymptotic regime starts at  $t \approx 1$  ps, corresponding to  $t \approx 3 \tau_{\text{VACF}}$ . On account of relation Eq. (5), this time scale also defines the onset of the asymptotic regime of the MSD. Since  $\tau_{\text{VACF}}$  is much smaller than the time scale on which the MSD varies notably, expression (1) can be in practice fitted for the whole time scale,  $0 \leq t < \infty$ . This has been tacitly assumed in the fits of the MSDs described earlier.

To compute the memory function, we started from the discretized form of Eq. (4),

$$\frac{c(n+1) - c(n)}{\Delta t} = - \sum_{k=0}^n \Delta t w_k c(n-k) \kappa(k), \quad (12)$$

where  $w_0 = w_n = 1/2$  and  $w_k = 1$  for  $k = 1, \dots, n-1$  (Simpson integration scheme). Equation (12) can be considered as a linear system of equations for  $\kappa(0), \kappa(1), \kappa(2), \dots$ , which can be solved recursively. The result is shown in Fig. 5, where the inset shows the long-time tail (dots) together with the analytical form (7) (solid line). Although the memory function decays very rapidly to almost zero compared to its initial value, it is exactly the remaining positive long-time tail which makes the diffusion process subdiffusive. We note that the agreement between the long-time tail of the memory function and the theoretical prediction is less good as for the VACF. A reason might be that the memory function is not well resolved for short times and that errors in the VACF are accumulated through the recursive calculation of  $\kappa(n)$ . The typical time scale for the memory function can be defined along the



same lines as for the VACF, using that<sup>20</sup>

$$\eta_\alpha = \frac{\langle v^2 \rangle}{D_\alpha} = \int_0^\infty dt {}_0d_t^{1-\alpha} \kappa(t). \quad (13)$$

Introducing the frequency  $\Omega \equiv \sqrt{\kappa(0)}$ , we define

$$\tau_{\text{mem}} = \left( \frac{\eta_\alpha}{\Omega^2} \right)^{1/\alpha}. \quad (14)$$

Using the same parameters as for the calculation of  $\tau_{\text{VACF}}$  and that  $\Omega^2 = 163.25 \text{ ps}^{-2}$ , we obtain  $\tau_{\text{mem}} = 2.7 \text{ fs}$ . This value confirms the very rapid decay of  $\kappa(t)$  seen in Fig. 5 and one sees that the asymptotic regime starts approximately at  $t \approx 10 \text{ ps}$ , which corresponds to  $t \approx 4000 \tau_{\text{mem}}$ . Although the characteristic time scale of the memory function is much shorter than the one of the VACF, its asymptotic regime starts even later.

To resume the results, we have shown that the lateral diffusion of the lipid molecules in the simulated DOPC bilayer displays a clear signature of subdiffusion, with fractional diffusion constants that are compatible with experimental results obtained by FCS. The asymptotic forms of the VACF and the corresponding memory function agree in particular with corresponding theoretical expressions predicted for this type of anomalous diffusion. It is worthwhile noting that the long-time tail  $\propto t^{\alpha-2}$  of the lateral VACF might have an explanation in terms of a hydrodynamic backflow of the surrounding molecules. This argument has been put forward long time ago to explain the long-time tails in the VACFs of simple liquids.<sup>19</sup> In this context, we refer to recent work by Falk *et al.*<sup>23</sup> who observed collective flow patterns in the lateral motions of molecules in a lipid bilayer.

<sup>1</sup>A. Einstein, *Ann. Phys.* **322**, 549 (1905).

<sup>2</sup>R. Metzler and J. Klafter, *Phys. Rep.* **339**, 1 (2000).

<sup>3</sup>P. Schwille, U. Haupts, S. Maiti, and W. Webb, *Biophys. J.* **77**, 2251 (1999).

<sup>4</sup>P. Schwille, J. Korlach, and W. Webb, *Cytometry* **36**, 176 (1999).

<sup>5</sup>L. Wawrezynieck, H. Rigneault, D. Marguet, and P.-F. Lenne, *Biophys. J.* **89**, 4029 (2008).

<sup>6</sup>K. Ritchie, X.-Y. Shan, J. Kondo, K. Iwasawa, T. Fujiwara, and A. Kusumi, *Biophys. J.* **88**, 2266 (2008).

<sup>7</sup>J.-H. Jeon, V. Tejedor, S. Burov, E. Barkai, C. Selhuber-Unkel, K. Berg-Sørensen, L. Oddershede, and R. Metzler, *Phys. Rev. Lett.* **106**, 048103 (2011).

<sup>8</sup>A. Weigel, B. Simon, M. Tamkun, and D. Krapf, *Proc. Natl. Acad. Sci.* **108**, 6438 (2011).

<sup>9</sup>S. Burov, J.-H. Jeon, R. Metzler, and E. Barkai, *Phys. Chem. Chem. Phys.* **13**, 1800 (2011).

<sup>10</sup>E. Fleener, J. Das, M. Rheinstädter, and I. Kosztin, *Phys. Rev. E* **79**, 11907 (2009).

<sup>11</sup>J. Wohler and O. Edholm, *J. Chem. Phys.* **125**, 204703 (2006).

<sup>12</sup>R. Zwanzig, *Nonequilibrium Statistical Mechanics* (Oxford University Press, New York, 2001).

<sup>13</sup>D. V. D. Spoel, E. Lindahl, B. Hess, G. Groenhof, A. E. Mark, and H. J. C. Berendsen, *J. Comput. Chem.* **26**, 1701 (2005).

<sup>14</sup>U. Essmann, L. Perera, M. L. Berkowitz, T. Darden, H. Lee, and L. G. Pedersen, *J. Chem. Phys.* **103**, 8577 (1995).

<sup>15</sup>J.-P. Ryckaert, G. Ciccotti, and H. Berendsen, *J. Comput. Phys.* **23**, 327 (1977).

<sup>16</sup>N. Kucerka, S. Tristram-Nagle, and J. F. Nagle, *J. Membr. Biol.* **208**, 193 (2005).

<sup>17</sup>H. Berendsen, J. Postma, W. van Gunsteren, A. DiNola, and J. Haak, *J. Chem. Phys.* **81**, 3684 (1984).

<sup>18</sup>J.-H. Jeon and R. Metzler, *J. Phys. A: Math. Theor.* **43**, 252001 (2010).

<sup>19</sup>J. Boon and S. Yip, *Molecular Hydrodynamics* (McGraw Hill, New York, 1980).

<sup>20</sup>G. Kneller, *J. Chem. Phys.* **134**, 224106 (2011).

<sup>21</sup>*NIST Handbook of Mathematical Functions*, edited by F. W. J. Olver, D. W. Lozier, R. F. Boisvert, and C. W. Clark (Cambridge University Press, Cambridge, England, 2010).

<sup>22</sup>K. Oldham and J. Spanier, *The Fractional Calculus* (Academic, New York, 1974).

<sup>23</sup>E. Falck, T. Róg, M. Karttunen, and I. Vattulainen, *J. Am. Chem. Soc.* **130**, 44 (2008).